Optik 125 (2014) 1248–1251

Contents lists available at ScienceDirect

Optik

journal homepage: www.elsevier.de/ijleo

Research of a sphere–cone window with good aberration characteristic

Chao Wang[a,b,*], Xin Zhang[a], He-Meng Qu[a], Ce Song[a,b]

[a] Key Laboratory of Optical System Advanced Manufacturing Technology, Changchun Institute of Optics, Fine Mechanics and Physics, Chinese Academy of Sciences, Changchun 130033, China
[b] University of Chinese Academy of Sciences, Beijing 100039 China

ARTICLE INFO

Article history:
Received 30 March 2013
Accepted 31 July 2013

Keywords:
Special optical window
Sphere–cone window
Aberration characteristic
Optical design
Super wide field-of-regard

ABSTRACT

Optical windows with external surfaces that shaped to satisfy operational environment needs are known as special windows. A novel special window, sphere–cone (SC) window, is presented. The equations used to decide geometrical parameters of this window are deduced. A SC MgF_2 window with a fineness ratio (F) of 1.33 is designed as an example. The field-of-regard (FOR) angle is ±80°. From the window system simulation results by the calculated fluid dynamics (CFD) and optical design software, we find that the SCP shape compared to conventional window forms not only introduces relatively less drag in the airflow, but also makes the minimal effect to imaging. After a correcting lens is adopted in the SC window optical system, the lowest modulation transfer function (MTF) value at 17 Lp/mm reaches 0.610 and the root-mean-square (RMS) spot size is approximately 1.57–2.12 times than the diffraction limit. The design results show that the SC window optical systems can achieve high image quality across very wide FOR by the simplest static correction.

1. Introduction

A special optical window/dome refers to the one whose outer shape conforms to the body of the vehicle to meet the aerodynamic requirements. At present, special window optics, with its excellent dynamic performance, wide FOR, and flexibility in determining where sensors will be housed in windows, is drawing increasing attention, and will be widely adopted in various types of aircraft [1]. The shape of the special window might be an aspheric formula that produces a higher fineness ratio (F) than the sphere [2,3]. The high F value is benefit to reduce the drag suffered by the vehicle in the airflow.

The influence on imaging is also a key factor in designs of special optical windows. The ellipse is the most prevalent form of the special window; however, this profile will induce severe non-central symmetry aberrations when the optics after the window is scanning across FOR [4]. In order to overcome this problem, complex aberration correcting methods will be adopted, which greatly augment the size, weight and cost of the whole system [5–7]. So there is a need for a novel window shape, which improves the aerodynamic performance with producing minimal wavefront distortion across super wide FOR to keep the configuration of the whole window optical systems simple and easy to fabricate. Chen et al. put forward a torus contour to reduce aberrations induced by the window, but the influence of this shape on the aerodynamic performance was not considered [8].

In this paper, a novel window having a sphere–cone (SC) shape is proposed. The formulas of the SC surface are given, and the equations that are used to decide geometrical parameters of this surface are deduced. Then, a SC window instance is given, and the drag and aberration characteristics of it are studied and compared to windows of traditional shapes with identical diameters. A single correcting lens successfully eliminates the imaging effect of the window. The analysis and design results confirm that the SC window not only improves the aerodynamic property of the aircraft, but also makes the optical correcting method extremely simplified so the system will be simple and lightweight for fitting the rigorous working environment.

2. Expression and structure parameter design of the SC surface

2.1. Formulas of the SC surface

Both front and back surfaces of the SC window are SC surfaces. The SC surface is a complex aspheric surface, whose sag is defined

* Corresponding author at: Key Laboratory of Optical System Advanced Manufacturing Technology, Changchun Institute of Optics, Fine Mechanics and Physics, Chinese Academy of Sciences, Changchun 130033, China.
E-mail address: Nicklo19992009@163.com (C. Wang).

0030-4026/$ – see front matter © 2013 Elsevier GmbH. All rights reserved.
http://dx.doi.org/10.1016/j.ijleo.2013.07.133

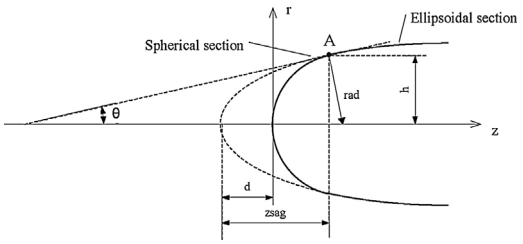

Fig. 1. Schematic diagram of a sphero-conical surface.

in polar coordinates by:

$$Z_{sag} = \begin{cases} \dfrac{c\rho^2}{1+\sqrt{1-c^2\rho^2}} & (\rho \le h) \\ \dfrac{c\rho^2}{1+\sqrt{1-(1+k)c^2\rho^2}} - d & (\rho > h) \end{cases} \quad (1)$$

where c denote the curvature, ρ and θ are radial coordinates, k is the conic constant and d is a axial translation amount for keeping the spherical and conical segments of the surface tangent to each other.

The schematic diagram of a SC surface is shown in Fig. 1. The rear section of the surface is a rear portion of an ellipsoid in this paper. The front portion of the ellipsoid, which length (distance from the vertex to the center of the base) is z_{sag}, is replaced by a spherical crown. The ellipsoidal section is tangent to the spherical section at the intersection line of them.

2.2. Derivations of equations for geometric parameter design

From Fig. 1, the length of the stitched surface reduces d compared with the original ellipsoid. *Rad* is the radius of the spherical section, and θ is the angle between the tangent plane of the surface at an intersection point A and z-axis. By the laws of geometry, the following equation can be obtained:

$$d = z_{sag} - rad * (1 - \sin\theta), \quad (2)$$

The general equation of the conical surface is shown as following:

$$z = \frac{cr^2}{1+\sqrt{1-(1+k)c^2r^2}}, \quad (3)$$

The base semi-diameter of the cut portion of the ellipsoid is h, so the following equation can be derived:

$$rad = h\sqrt{1+(\tan\ \theta)^2}, \quad (4)$$

Substituting h for r in Eq. (3), z_{sag} can be obtained:

$$z_{sag} = \frac{ch^2}{1+\sqrt{1-(1+k)c^2h^2}}, \quad (5)$$

From Eq. (3), the value of $\tan\theta$ can be obtained:

$$\tan\theta = \frac{dr}{dz}|_{r=h} = \frac{\sqrt{1-(1+k)c^2h^2}}{ch}, \quad (6)$$

According to the trigonometric function operation and Eq. (6), the value of $\sin\theta$ can be solved:

$$\sin\theta = \sqrt{\frac{\tan\theta^2}{\tan\theta^2+1}}. \quad (7)$$

Using Eqs. (1)–(7), the length d can be solved numerically. If the length of the original uncut ellipsoid is L, the length of the stitched window is L' and the diameter is D, the fineness ratio (length to diameter ratio) of the stitched window will be:

$$F = \frac{L'}{D} = \frac{L-d}{D}. \quad (8)$$

Table 1
SC window design parameters.

Fundamental design parameters	Outer surface	Inner surface
Curvature of the original ellipsoid, c	0.0800 mm^{-1}	0.07874 mm^{-1}
Conic constant of the original ellipsoid, k	−0.9375	−0.9164
Length of the original ellipsoid, L	200 mm	196 mm
Semi-diameter of the spherical section, h	44 mm	40.4696 mm
Thickness of the window, t	4 mm	
Diameter of the window, D	100 mm	
Length of the stitched window, L'	133.4563 mm	
Fineness ratio of the stitched window, F	1.33	

2.3. The baseline SC window

It is necessary to define a particular SC window for following detailed discussions. The modeling of the window is accomplished through the selection of fundamental design parameters, as shown in Table 1.

3. Analysis of aerodynamic performance and aberration characteristic of the SC window

To quantitatively explain the strong points of SC window, the familiar ellipsoidal window will be chosen for the control one in analysis of aerodynamic and imaging performance.

3.1. The drag coefficients

We will make a contrast simulation experiment on aerodynamics between different window shapes. Experiment objects consist of a SC window which parameters are given in Table 1, a fineness ratio (F) 0.75 ellipsoidal window and a hemispherical window. The diameter of each window is 100 mm. Fig. 2 displays geometries of these windows. The base of each window is connected to one end face of a 100 mm diameter, 700 mm length cylinder, as the aircraft models in the CFD simulation. We divide the 3D flow field around the model into unstructured mesh elements, and adopt the solver based density, Spalart–Allmaras viscous model and pressure far field boundary [9]. The speed of aircraft is 3*Ma*. Simulation with each model is conducted under above conditions. The drag coefficients of the windows are shown in Table 2. Obviously, compared with the conventional spherical window, there is an aerodynamic benefit in going to the SC and ellipsoidal windows.

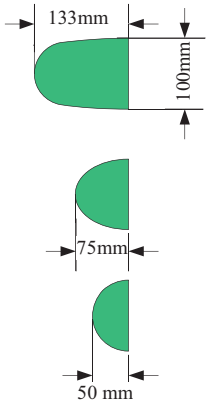

Fig. 2. Window structures of the contrast simulation.

Table 2
Drag coefficients for different window shapes.

Window shape	Drag coefficient
Hemisphere	9.5378e−01
F 0.75 ellipsoid	7.5548e−01
F 1.33 SC	7.8654e−01

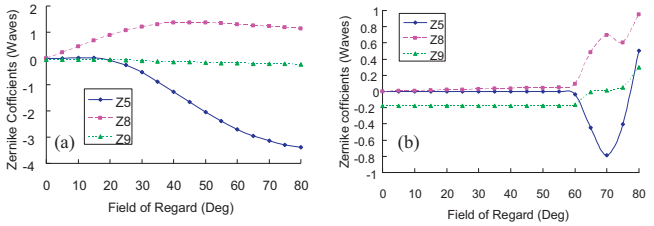

Fig. 3. Zernike aberrations versus look angle: (a) *F* 0.75 ellipsoidal window (b) *F* 1.33 sphero-conical window.

The *F* 0.75 ellipsoidal window introduce about 0.8 time drag than the hemisphere window, and this result coincides with data in published literature [10]. Drag produced by the *F* 1.33 SC window is approximately same with the ellipsoidal window.

3.2. Aberration characteristics

Then, aberration characteristics of the SC window will be analyzed and compared to the ellipsoidal window. The *F* 1.33 stitched window and *F* 0.75 ellipsoidal window studied in the above CFD simulation are chosen for typical examples. The *F* 0.75 window is with a thickness of 4 mm, a diameter of 100 mm and a inner ellipsoidal surface with a fineness ratio of 0.75 and a diameter of 92 mm. For each of the two windows, the system wavelength range is 3–5 μm, the window material is MgF_2, the entrance pupil diameter is 35 mm and the imaging system is a perfect lens gimballing behind the window, which has a 40 mm focal length and a half angle range of 80° from boresight to the edge of FOR. The perfect lens is located at 44.3988 mm behind the outer surface. As is customary, we characterize aberrations of the windows by decomposing the wavefront at the exit pupil into Zernike polynomials [5]. Fig. 3 shows plots of aberrations versus the look angle. The dominant aberrations caused by the window are 3rd order spherical aberration (Z_9), coma (Z_8) and 3rd order astigmatism (Z_5).

It can be seen from Fig. 3 that the peak-to-valley of the Zernike aberrations for the *F* 0.75 window is much larger than the *F* 1.33 window. For the *F* 1.33 window, the amount of aberrations almost does not vary with look angle when the angle is no more than 55°. This is due to the optical system images through the spherical section of this window and the axis of rotation is at the center of curvature of this section. When the FOR angle is between 55° and 80°, one portion of light rays pass through the conical section of the window. The two window sections introduce different amounts of optical power, leading considerable astigmatism and coma in the wavefront of the exit pupil. But the aberrations are still on the order of one wave.

4. Aberration correction and system optimization

For the *F* 1.33 element, almost constant spherical aberration is the predominant aberration when FOR angle is no more than 55°, which can be compensated by the actual imaging lens group. Beyond 55°, a transparent correcting lens is utilized to eliminate image effect of the conical portion, as shown in Fig. 4. The combined conical portion and corrector will have the same optical power as the ellipsoidal portion, so focus is maintained. The corrector was

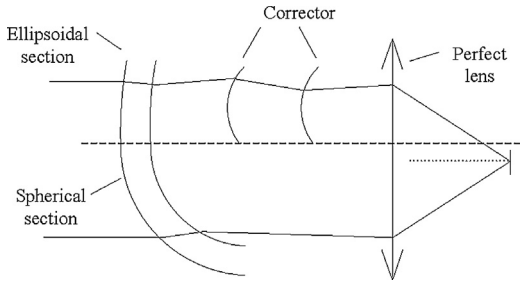

Fig. 4. Schematic diagram of the window optical system with a correcting lens.

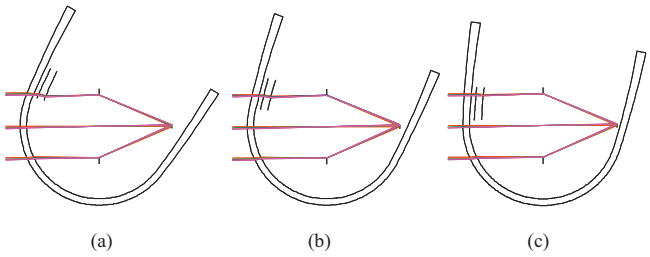

Fig. 5. The final system layouts at FOR angles: (a) 60°; (b) 70°; (c) 80°.

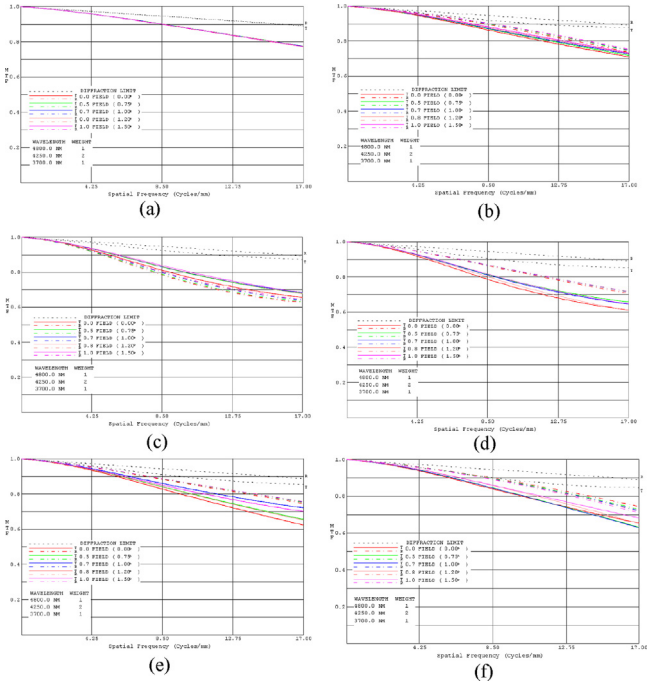

Fig. 6. MTF plots of the ultimate system at FOR angles: (a) 55°; (b) 60°; (c) 65°; (d) 70°; (e) 75°; (f) 80°.

designed with two aspheric surfaces. The optical system is optimized over the full FOR of 80°, and a 3° instantaneous field of view (IFOV) is added. The final system layouts at typical FOR angles are shown in Fig. 5.

In the actual application, there will be two identical corrector lenses. The locations of these two lenses are symmetric in the inner space of the window. The imaging system should employ the catadioptric configuration to reduce system volume for leaving enough space for the corrector lenses.

Fig. 6 is MTF curves of the final system. The MTF values of every look angle reach or surpass 0.610 at 17 Lp/mm. The MTF plots at 0–50° field angles are nearly identical to the MTF plot at 55°, so these figures are omitted. Fig. 7 shows the RMS spot size of each

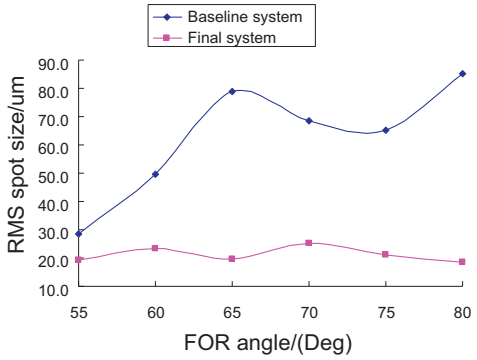

Fig. 7. RMS spot sizes of the baseline system and the final corrected system.

look angle. The top line shows the spot size for the SC system without any correction. The bottom line shows the spot size for the corrected system. For comparison, the corrected system spot size is 19–25 μm, which is approximately 1.57–2.12 times the diffraction limit. The results show that the aberrations induced by the window can be successfully decreased by inserting the fixed corrector into the system.

5. Conclusions

According to the present invention, we validate that the SC window shape alleviates the air resistance of the vehicle with producing a very small amount of aberrations across super wide FOR angles. An optical corrector with a minimum number of optical surfaces is enough to compensate these aberrations. Taking engineering application into consideration, the application of SC windows will simplify the aberration correction device and omit the extra servomotors usually adopted in the airborne special window/dome optical system, which will significantly reduce the weight and volume and enhance the reliability of the system.

Acknowledgment

This research is supported by the Young Scientists Fund of the National Natural Science Foundation of China (No. 61007009).

References

[1] J.P. Mills, Conformal optics: theory and practice, Proc. SPIE 4442 (2001) 101–107.
[2] D.J. Knapp, Fundamentals of conformal dome design, Proc. SPIE 4832 (2002) 394–409.
[3] J.D. Nelson, A. Gould, D. Dworzanski, C. Klinger, B. Wiederhold, M. Mandina, Rapid optical manufacturing of hard ceramic conformal windows and domes, Proc. SPIE 8016 (2011) 80160O.
[4] B.G. Crowther, D.B. McKenney, J.P. Mills, Aberrations of optical domes, Proc. SPIE 3482 (1998) 48–61.
[5] D.L. Song, J. Chang, Q.F. Wang, W.B. He, J. Cao, Conformal optical system design with a single fixed conic corrector, Chin. Phys. B 20 (2011) 074201.
[6] C. Wang, X. Zhang, H.M. Qu, G.W. Shi, L.J. Wang, Design of novel catadioptric elliptical dome optical system, Acta Optic. Sin. 32 (2012) 0822002.
[7] T.A. Mitchell, J.M. Sasian, Variable aberration correction using axially translating phase plates, Proc. SPIE 3705 (1999) 209–220.
[8] Chen et al., Optical system having a generalized torus optical corrector, US Patent 5914821 (June 22, 1999).
[9] Fluent Inc., FLUENT 6.3 User's Guide (2006).
[10] Q. We, X.Q. Ai, Optimizing design of dome figure for supersonic seekers, 0pt, Precision Eng. 18 (2) (2010) 384–389.